ISSN: 0976-3031

Available Online at http://www.recentscientific.com

CODEN: IJRSFP (USA)

International Journal of Recent Scientific Research
Vol. 10, Issue, 05(B), pp. 32283-32289, May, 2019

International Journal of Recent Scientific Research

DOI: 10.24327/IJRSR

Research Article

SYNTHESIS OF POLY P-AMINOPHENOL/TIO_2 COMPOSITE IN THE PRESENCE OF ANIONIC SURFACTANTS AND THE INVESTIGATION OF ANTICORROSION PROPERTIES

G. Thenmozhi[1] and Jaya Santhi R[2]

[1]Department of Chemistry, Arcot Sri Mahalakshmi Women's College, Vellore-632521, Tamil Nadu, India
[2]Department of Chemistry, Auxilium College, Vellore-632006, Tamil Nadu, India

DOI: http://dx.doi.org/10.24327/ijrsr.2019.1005.3437

ARTICLE INFO

Article History:
Received 15th February, 2019
Received in revised form 7th March, 2019
Accepted 13th April, 2019
Published online 28th May, 2019

Key Words:

Aminophenol, Polymerization, Titanium dioxide, Anti corrosion, Mild steel.

ABSTRACT

"In situ" polymerization was carried out in the presence of TiO2 to synthesize polypara aminophenol/ TiO2 (PpAP/TiO2) composite using anionic surfactants DBSA and SDS at 0˚C and characterized by FTIR, UV–VIS-NIR spectroscopy, XRD and TGA. The corrosion protection performances of composites on Mildsteel in 1M HCl solution were evaluated using Potentiodynamic polarization and Electrochemical impedance spectroscopy measurements. These measurements reveal that the inhibition efficiency increased by increasing their concentration. Polarization studies reveal that composites act as a mixed type corrosion inhibitor. It was found that this inhibitor acts through adsorption on the metal surface and obeys Langmuir adsorption isotherm.

INTRODUCTION

Organic and inorganic composites have attracted considerable attention as they can combine the advantages of both components and may offer special properties through reinforcing or modifying each other (Nandapure *et.al*.,2013). To improve and extend the functions of the conducting organic materials, inorganic materials such as metals and metal oxides are often incorporated to form multi-functionalized composites for various applications in the fields of electronics, sensors, catalysis, energy, electromagnetic interference shielding and biomedicine (Nandapure *et.al*.,2012). Recently, the use of conducting polymers for the protection of metals against corrosion has been investigated. Unlike anilineand other substituted anilines, amino phenols present two oxidizable groups (NH_2 and OH) providing more reactive sites (Odonírio Abrahão,2009). Recently, poly aminophenol has attracted considerable attention for the preparation of its composites with inorganic particles in the presence of surfactants to improve their processability.

Mild Steel (MS) is one of the important iron-containing alloys used in many industrial aqueous systems in which water circulates. The use of inhibitors is one of the most practical methods for protection against corrosion in closed systems, especially in acidic media (Chetouani, 2004;Tebbji *et.al*.,2007). Organic compounds are widely used as corrosion inhibitors in acidic environments in various industries (Ebenso,2005;Kern,2001). Their role as barrier on metal surface and to prevent the access of corrosive environment to metal substrate is well known to reduce the corrosion rate.

In the present work, PpAP/TiO_2 composites were prepared in the presence of two anionic surfactants like DBSA and SDS by chemical oxidation method and characterized by different spectroscopic techniques. An attempt has been made to investigate the corrosion protection behaviour of chemically synthesised PpAP/TiO_2-DBSA and PpAP/TiO_2-SDS composites over MS in acidic environment using potentiodynamic polarisation and electrochemical impedance spectroscopy (EIS) measurements.

EXPERIMENTAL METHOD

Synthesis of PpAP/TiO_2 Composites

The equimolar volumes of 0.1 M solution of para aminophenol and HCl were prepared in double distilled water, mixed and kept in the freezing mixture. 2g TiO_2 of was added to the above solution and kept for vigorous stirring to keep the TiO_2 suspended in the solution. 0.1 M ammonium per sulphate and

Corresponding author:* **G. Thenmozhi
Department of Chemistry, Arcot Sri Mahalakshmi Women's College, Vellore-632521, Tamil Nadu, India

0.025 M DBSA were taken in separate beakers. The oxidant and surfactant were added slowly to the mixture containing para aminophenol and TiO_2 and the stirring was continued for six hours at 0˚C. The product was filtered, washed with excess amount of water, methanol and acetone to remove excess of HCl, APS and DBSA. The resulting composite was then dried at 50˚C for 24h. The same procedure was adopted for the synthesis of PpAP- TiO_2/SDS Composite.

Characterization

UV-VIS-NIR spectra of composites dissolved in DMSO solvent was obtained using Varian, Cary-5000 spectrophotometer in the range of 200-2500 nm. The FT-IR spectrums were recorded by Thermo Nicolet, Avatar 370 Spectrophotometer. The spectrum of the dry polymer powder in KBr pellet was recorded from 500cm^{-1} to 4000cm^{-1}. X-ray diffraction (XRD) scan was done with Bruker AXS D8 Advance diffractometer at room temperature using Cu Kα (λ=1.5406 A˚). Thermo gravimetric analysis (TGA) was carried out in nitrogen atmosphere at a heating rate 10˚C/min up to 750˚C temperature by Perkin Elmer, Diamond TG/DTA analyzer.

Electrochemical measurements, including potentiodynamic polarization curves and Electrochemical Impedance Spectroscopy (EIS) were performed in a conventional three electrode cell using a computer-controlled potentiostat /galvanostat (Autolab PGSTAT 302N potentiosat from Eco-chemie, Netherlands). Platinum electrode was used as the counter electrode, Ag/AgCl, 3M KCl as the reference electrode and the mild steel specimen was used as a working electrode. Specimen of dimension 1x1x 0.1 cm was used for electrochemical studies. The specimens were embedded in epoxy resin leaving a working area of 1 cm^2. The surface preparation of the mechanically abraded specimens was carried out by using different grades of silicon carbide emery paper (up to 1200 grit) and subsequent cleaning with acetone and rinsing with double distilled water was done before each experiment
Before each potentiodynamic polarization (Tafel) and EIS studies, the electrode was allowed to corrode freely and its open circuit potential (OCP) was recorded as a function of time up to 20 min, which was sufficient to attain a stable state. After this, a steady-state of OCP corresponding to the corrosion potential (E_{corr}) of the working electrode, was obtained. The potentiodynamic measurements were started from cathodic to the anodic direction, E = E_{corr} ± 250 mV, at a scan rate of 10 mVs^{-1}. The linear Tafel segments of the anodic and cathodic curves were extrapolated to obtain E_{corr} and corrosion current density (I_{corr}). The inhibition efficiency was evaluated from the measured I_{corr} with and without inhibitor using the relationship,

$$IE\ (\%) = \frac{I^{\circ}_{corr} - I_{corr}}{I^{\circ}_{corr}} \times 100 \qquad (1)$$

where I^{0}_{corr} is the corrosion current density without inhibitor and I_{corr} is the corrosion current density with inhibitor. The corrosion rates (CR) of MS with polymers were calculated from polarization curves using the following equation (Srikanth,2007).

$$CR = \frac{3.27 \times 10^{-3} \times I_{corr} \times EW}{D} \qquad (2)$$

where CR is the corrosion rate (mmpy), I_{corr} is the corrosion current density (μA cm^{-2}), EW is the equivalent weight of the specimen, and D is the density (g cm^{-3}) of the specimen, respectively.

EIS measurements were carried out using AC signals of 10 mV for the frequency spectrum from 100 kHz to10 mHz at the stable OCP. The potentiodynamic polarization and EIS data were analyzed and fitted using graphing and analyzing impedance software, Nova 1.4. Fresh solution and fresh steel samples were used after each sweep. The charge transfer resistance (R_{ct}) was obtained from the diameter of the semicircle of the Nyquist plot. The inhibition efficiency of the inhibitor has been found out from the charge transfer resistance values using the following equation

$$IE\ (\%) = \frac{R_{ct} - R^{\circ}_{ct}}{R_{ct}} \times 100 \qquad (3)$$

where R^{0}_{ct} and R_{ct} are the charge transfer resistance in the absence and in the presence of the inhibitor.

RESULTS AND DISCUSSION

UV-VIS-NIR Spectroscopy

The UV-VIS-NIR absorption spectrums of PpAP and TiO_2composites dissolved in DMSO are shown in Figure 1.

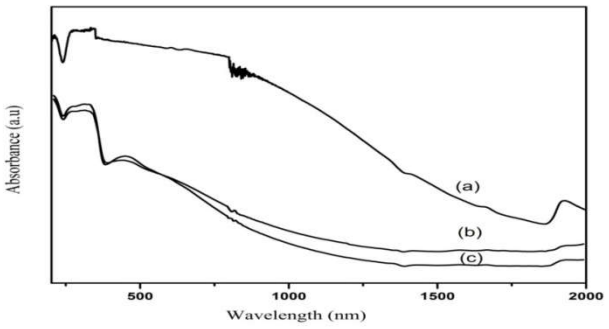

Figure 1 UV-VIS-NIR Spectra of (a) PpAP (b) PpAP/TiO_2-SDS and (c) PpAP/TiO_2-DBSA

These spectrum consist of two major absorption peaks, the first peak around 312 nm is assigned to the π − π* transition of the phenyl rings which is related to the extent of conjugation between the phenyl rings in the polymer chain and composites. The intensity of the $\pi - \pi^*$ absorption maxima is comparable for these synthesized composites in the presence of anionic surfactants. The second absorption peak at 452 nm is assigned to n-π* transition between the HOMO orbital of the benzenoid ring and the LUMO orbital of the quinoid ring (Elmansouri,2009). The peak around 1420 nm has been assigned to $-NH_2^+$ species which is generated on doping or the polaronic transitions. From comparison of UV–vis spectra PpAP and PpAP/TiO_2 composites can be seen that, the shapes of peaks were very similar, but there are some shifts due to the strong interaction between PpAP and TiO_2 particles.

FT-IR Analysis

The representative FT-IR spectrum of PpAP and TiO_2 composites are given in Figure 2. The main characteristic peaks of PpAP can be interpreted as: the broad intense peak around 3219 cm^{-1} is assigned to O–H stretching vibrations. A shoulder peak at 1504 cm^{-1} is due to stretching vibrations of N–H in secondary amine, indicates that the polymerizing chains grow through the amino groups. Two main peaks around 1600 and 1560cm^{-1} in the spectrum corresponds respectively to the ring-stretching vibrations of the quinoid and benzenoid rings (Thenmozhi,2014). The presence of these two rings clearly shows that polymer is composed of the amine and imine units. The peak appears around 2362 cm^{-1} which is the characteristics stretching band for C = C = N or C = C = O (Kar,2010).

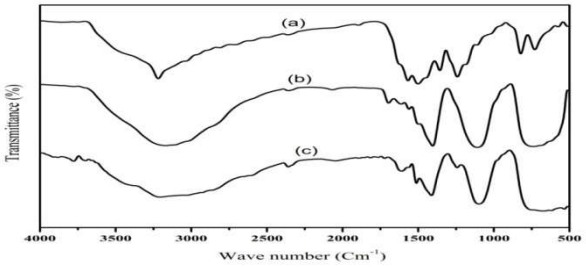

Figure 2 FT-IR Spectra of (a) PpAP (b) PpAP/TiO_2-SDS and (c) PpAP/TiO_2-DBSA

The FTIR spectrum of PpAP/TiO_2 composites synthesized in two anionic surfactants are identical to PpAP but all the peaks of PpAP/TiO_2 composites shift slightly to the lower frequencies. Composites show two additional peak at 1699 cm^{-1} and 1107 cm^{-1} corresponds to Ti – O- C stretching mode in each case (Yang,2005) and the broad peak in the region between 400 and 850 cm^{-1} is attributed to the characteristic strong absorbance of TiO_2 due to the formation of an O–Ti–O network (Nag,2007).The FTIR study confirms that the TiO_2 molecules are well incorporated with PpAP structure. It can be concluded that there is an interaction between PpAP macromolecule and TiO_2 particles. The interaction may be associated with the interaction of titanic and nitrogen atom in PpAP macromolecule. Titanium is a transition metal, has intense tendency to form coordination compound with nitrogen atom in PpAP. All above results suggest that it is not a simple blend or mix between PpAP and TiO_2, but rather an interaction exists at the interface of PpAP and TiO_2 particles (Zhitao Li *et.al*.,2013).

XRD Analysis

Figure 3shows the XRD pattern of TiO_2, PpAP and PpAP/TiO_2composites. PpAP exhibits broad Bragg diffraction peaks at 2θangles of 17.6˚, 19.4˚, 24.2˚ and 25.5˚, 2Θ= 25.5˚ is characteristics of the van der Waals distances between stacks of phenylene rings (poly aminophenol rings) (Thenmozhi *et.al*.,2014). These strongest peaks indicate crystalline domains in the amorphous structure of the polymers. It can be seen that the XRD patterns of PpAP/TiO_2-DBSA and PpAP/TiO_2-SDS are very much similar to that of TiO_2 and the broad diffractive peak of PpAP has become weak. It is because when PpAP absorbed on the surface of TiO_2 particles, the molecular chain of PpAP was confined and the degree of crystallinity decreased. It also confirms that the PpAP deposited on the surface of TiO_2 has no effect on the crystalline structure of TiO_2.

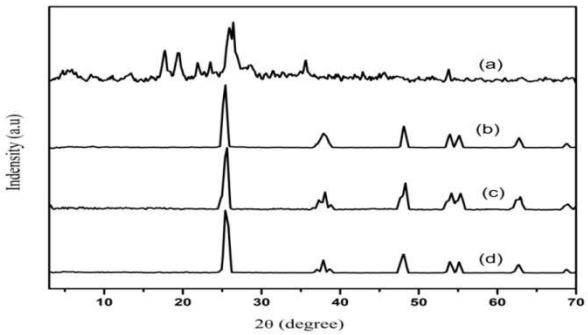

Figure 3 XRD Patterns of (a) PpAP (b) TiO_2 (c) PpAP/TiO_2-SDS and (d) PpAP/TiO_2-DBSA

Thermo Gravimetric Analysis

Thermal degradation pattern of the PpAP and PpAP/TiO_2 composites are displayed in Fig. 4.

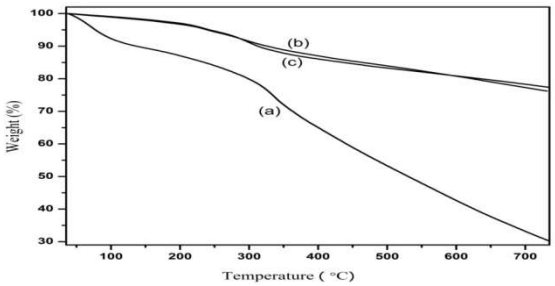

Figure 4 TGA curves of (a) PpAP (b) PpAP/TiO_2-SDS and (c) PpAP/TiO_2-DBSA

The TGA of PpAP and PpAP/TiO_2composites undergo three weight loss steps, the first step weight loss around 80˚C. It is known that PpAP and TiO_2 are hygroscopic and during the heating to 100˚C the residual water evaporates (Jia, *et.al*.,2002).The second weight loss around 290˚C is due to removal of HCl, sublimation and removal of low molecular weight polymer/oligomer. The third weight loss around 430˚C is due to decomposition of the polymer backbone in PpAP, removal of DBSA dopant (PpAP/TiO_2-DBSA) and SDS dopant (PpAP/TiO_2-SDS) in composites. The decomposition of PpAP is continuous upto 700˚C and even after 700˚C the complete decomposition has not taken place. The decomposition of PpAP and PpAP/TiO_2 composites leaves some char content. When compared with the TGA of PpAP/TiO_2 composites, it can be seen that the degradation of PpAP/TiO_2 composites is somewhat similar to that of PpAP. The noticeable difference is that the thermal decomposition of the composites starts at much lower temperature than that in pure PpAP, which may be due to the strong interaction between PpAP and TiO_2(Zheng,2008). The coordination between titanium and nitrogen atom probably weakened the interchain interactions in PpAP composites and helped the thermal degradation of composites. This is also clear from the XRD where sharp peak of PpAP disappeared in the composites probably due to the interaction of PpAP and TiO_2 resulting in the decreased thermal stability.

Potentiodynamic Polarization Studies

The potentiodynamic polarization curves of MS in 1M HCl with the addition of various concentrations of PpAP/TiO_2-DBSAand PpAP/TiO_2-SDS are shown in Figure 5a and b.

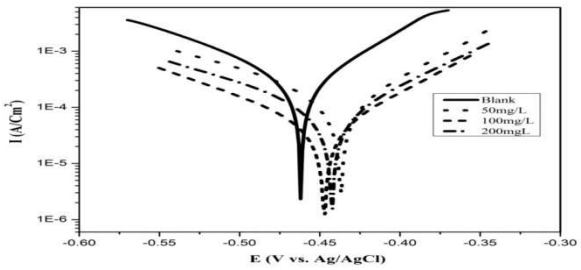

Figure 5a Potentiodynamic polarization curves obtained for Mild steel in 1M HCl in the presence and absence of different concentrations of PpAP/TiO_2-DBSA

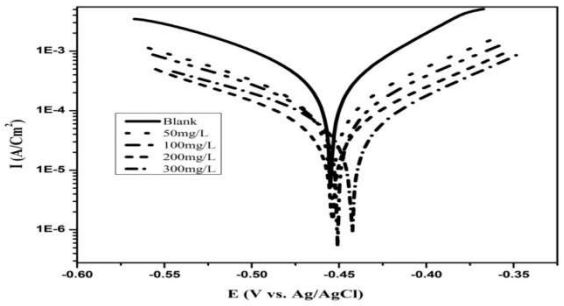

Figure 5b Potentiodynamic polarization curves obtained for Mild steel in 1M HCl in the presence and absence of different concentrations of PpAP/TiO_2-SDS

The corrosion kinetic parameters such as I_{corr}, E_{corr}, anodic Tafel slope b_a and cathodic Tafel slope b_c, inhibition efficiency IE and CR deduced from the curves are given in Table 1.

E_{corr}, ba and bc values do not change appreciably with the addition of the inhibitors indicating that the inhibitors are not interfering with the anodic dissolution or cathodic hydrogen evolution reactions independently but acts as a mixed type of inhibitor (Thenmozhi, 2014).These results confirm that the composites on MS act as a highly protective layer, which is mainly attributed to the presence of π electrons in aromatic ring coexisting with quaternary nitrogen atom and large molecular size (Evrim Hur *et.al*.,2007). The surface coverage is approximately 0.953 (PpAP/TiO_2-DBSA) and 0.962 (PpAP/TiO_2-SDS) which is good to act as a corrosive inhibitors.

Electrochemical Impedance Spectroscopy

The Nyquist plots of MS in 1M HCl in the presence and absence of various concentrations of PpAP/TiO_2 composites are depicted in Figure 6a and b respectively.

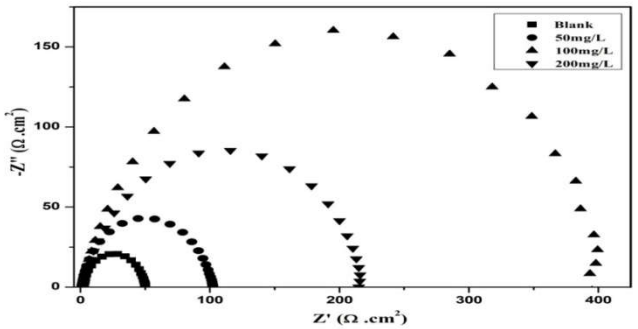

Figure 6a Nyquist plots obtained for Mild steel in 1M HCl in the presence and absence of different concentrations of PpAP/TiO_2-DBSA

Table 1 Potentiodynamic polarization parameters for Mild steel without and with different concentrations of PpAP/TiO_2 Composites in 1M HCl

Inhibitor concentration (mg/L)	b_a (mV/decade)	b_c (mV/decade)	E_{corr} (mV)	I_{corr} (μA/cm²)	IE (%)	Θ	CR (mm/Year)
			PpAP/TiO_2-DBSA				
Blank	56	44	461	3210	-		17.82
50	73	54	456	173	94.6	0.95	1.91
100	77	57	445	59	98.2	0.98	0.69
200	78	54	448	227	92.9	0.93	1.93
			PpAP/TiO_2-SDS				
Blank	54	75	454	3210	-		17.82
50	87	58	453	178	94.5	0.95	1.99
100	55	47	449	153	95.2	0.95	1.84
200	66	50	442	80	97.5	0.98	0.93
300	68	53	453	92	97.1	0.97	1.012

The I_{corr}values decreases from 3210μAcm^{-2} for the blank acid to 59 and 153 μAcm^{-2} for PpAP/TiO_2-DBSA and PpAP/TiO_2-SDS for the addition of 100mgL^{-1} two composites resulting in 98.2 and 95.2% of IE. It is clear that the I_{corr} values decreases with the presence of two composites indicated that composites are adsorbed on the metal surface and hence inhibition occurs. As the concentrations increases 50 to 200mgL^{-1} for PpAP/TiO_2-SDS the IE increases 94.5 to 97.5%, the further increase in concentration the IE value decreases. Similar trend has obtained in PpAP/TiO_2-DBSA and showed the maximum IE of 98.2% at 100mgL^{-1}. The high IE was due to the bonding of the adsorbed film of the inhibitor on the steel surface.The

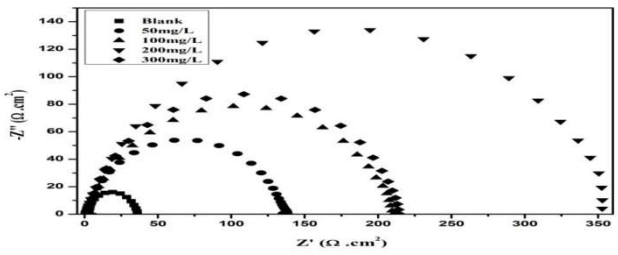

Figure 6b Nyquist plots obtained for Mild steel in 1M HCl in the presence and absence of different concentrations of PpAP/TiO_2-SDS

The Nyquist spectra obtained for blank showed depressed semicircle, representing the corrosion process of the system i.e., the charge transfer resistance due to the metal corrosion and the double layer capacitance of the liquid/metal interface. However, the Nyquist spectra of PpAP -TiO_2 composites at various concentrations showed depressed semicircle. The depressed semicircles in the Nyquist plots were probably due to the surface heterogeneity or corrosion products of the metal substrate. The element at high frequency region is related with the R_{ct} of system, elements at low frequency region may represent adsorption of ions, e.g. Cl^- which is the initial step of anionic or solvent exchange between polymers and solution during equilibration in 1M HCl (Bereket,2009).The electrochemical parameters derived from Nyquist plots are calculated and listed in Table 2.

Table 2 Impedance parameters for Mild steel in 1M HCl in the presence and absence of different concentrations of PpAP- TiO_2 Composites

Inhibitor concentration (mg/L)	C_{dl} (µF/cm^2)	R_{ct} (Ω Cm^2)	IE (%)	Θ
PpAP/TiO_2-DBSA				
Blank	7.28	38.68	-	-
50	6.85	100.73	61.6	0.616
100	5.02	405.04	90.45	0.905
200	6.69	213.23	81.86	0.819
PpAP/TiO_2-SDS				
Blank	7.28	38.68	-	-
50	6.95	149.63	74.15	0.742
100	6.43	226.02	82.88	0.829
200	2.34	376.96	89.74	0.897
300	4.84	232.46	83.36	0.834

The values of R_{ct} were given by subtracting the high frequency impedance from the low frequency one as follows (Ahmed,2013):

$R_{ct} = Z$`re (at low frequency) – $Z$`re (at high frequency)

The values of electrochemical double layer capacitance (C_{dl}) were calculated at the frequency, f_{max}, at which the imaginary component of the impedance is maximal ($-Z_{max}$) by the following equation:

$$C_{dl}=(2\pi f_{max}R_{ct})^{-1}$$

The impedance data listed in Table 2 indicate that the values of both R_{ct} and IE (%) are found to increase with increasing the inhibitor concentration, while the values of C_{dl} are found to decrease. This behavior was the result of an increase in the surface coverage by the inhibitor molecules, which led to an increase in the IE. The decrease in C_{dl} values may be considered in terms of Helmholtz model (Migahed *et.al*.,2011). The R_{ct} is increased from 20.12 Ω cm^2 for blank solution to 405.04 Ω cm^{2}upon addition of 100mg/L of PpAP/TiO_2-DBSA resulting in 90.45% IE but for PpAP/TiO_2-SDS the R_{ct} value increased to 376.96 Ω cm^{2}upon addition of 200mg/L resulting in 89.74% IE. The increase in R_{ct} value is attributed to the formation of an insulating protective film at the metal/solution interface [Bentiss,2000;Murlidharan*et.al*.,1995).For the two composites the effect is reversed with further increase in the concentration as seen in the result. As the concentration of the PpAP/TiO_2-DBSAincreased above 100mg/L, the corrosion resistance decreased. In fact, the highest IE was reached at 100mg/L for PpAP/TiO_2-DBSA and 200mg/L for PPAP/TiO_2-SDS which is considered to be an optimum inhibitor concentration of the synthezied composites. The decrease in C_{dl} values can result from a decrease in local dielectric constant and/or an increase in the thickness of the electrical double layer. It could be assumed that the decrease of C_{dl} values is caused by the gradual replacement of water molecules by adsorption of inhibitor molecules on the electrode surface, which decreases the extent of the metal dissolution. The Nyquist impedance plots were analyzed by fitting the experimental data to a simple equivalent circuit model given in Figure 7.

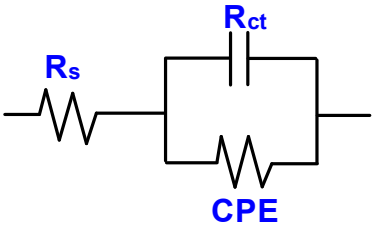

Figure 7 Equivalent circuit model used to fit the metal/solution interface.

In this equivalent circuit (Figure 7), $R_s$is the solution resistance, R_{ct} is the charge transfer resistance, and CPE is a constant phase element, which is placed in parallel to charge transfer resistance element. Thus, in these situations, pure double layer capacitors are better described by a transfer function with constant phase elements (CPE) to give a more accurate fit (Arockiasamy*et.al*.,2014) and its impedance is given by

$$Z = A^{-1} (i\omega)^{-n}$$

where A is proportionality coefficient, ω is the angular frequency, i is the imaginary number, and n is an exponent related to the phase shift and can be used as a measure of surface irregularity. For ideal electrodes, when n = 1, CPE can be considered as a real capacitor. The surface coverage is approximately 0.78(PpAP/TiO_2-DBSA)and 0.826 (PpAP/TiO_2-SDS) which is found to be good to act as an anticorrosive agent. The results obtained from EIS method is in good agreement with the linear polarization measurement.

The enhanced corrosion protection of MS by PpAP/TiO_2 composites can be explained on the basis of molecular adsorption. The composites inhibit corrosion by controlling both the anodic and cathodic reactions. In acidic solution, the composites molecules exist as protonated species (Gopalakrishnan Aridoss*et.al*.,2010). These protonated species adsorb on the cathodic sites of MS and decrease the evolution of hydrogen. The adsorption on anodic sites occurs through long π-electrons of aromatic rings (benzenoid and quinoid) and lone pair of electrons of nitrogen atoms, which decreases the anodic dissolution of MS (Quraishi,2000). It is well known that the species having high molecular weight and bulky structure may cover more area on the active electrode surfaces. The higher performance of the PpAP/TiO_2-DBSA than PpAP/TiO_2-SDS is due to the higher molecular size and high electron density on the adsorption centers.

Adsorption Isotherm

Several isotherms including Frumkin, Langmuir, Temkin, Freundlich, Bockris–Swinkels and Flory–Huggins isotherms are employed to fit the experimental data. It is found that the adsorption of studied PpAP/TiO_2 composites on the mild steel surface obeys Langmuir adsorption isotherm equation:

$C_{inh}/\theta = 1/K_{ads} + C_{inh}$ (7)

where, C is the concentration of inhibitor, K_{ads} the adsorptive equilibrium constant and θ is the degree surface coverage (θ = *IE%* / 100). The degree of surface coverage values for various concentrations of PpAP/TiO_2composites in the 1M HCl solution have been calculated from the average of inhibition efficiency of potentiodynamic polarization and EIS measurements (Table 1&2). Plots of C/θ against C yield straight lines as shown in Figure 8 and 9. Both linear correlation coefficient (r) and slope are close to 1, indicating the adsorption of the investigated inhibitors on the carbon steel surface obeys Langmuir adsorption isotherm. From this, it can conclude that the PpAP /TiO_2 composites can act as a good inhibitor.

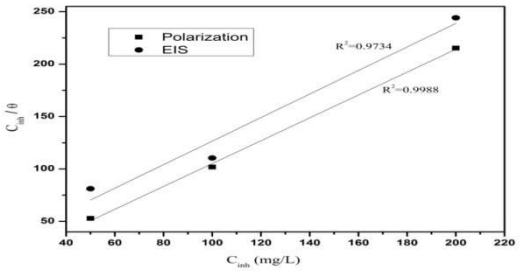

Figure 8 Langmuir adsorption isotherm for MS in 1M HCl solution of PpAP/TiO_2-DBSA composite at different concentrations

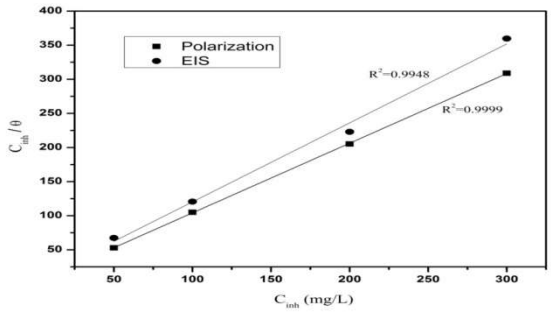

Figure 9 Langmuir adsorption isotherm for MS in 1M HCl solution of PpAP/TiO_2-SDS composite at different concentrations.

CONCLUSION

PpAP/TiO_2 composites were successfully synthesized using two surfactants DBSA and SDS at 0˚C.It can be concluded from different spectroscopic techniques that there is an interaction between PpAP and TiO_2 particles. Polarization curves demonstrated that the examined composites behave as a mixed type of inhibitors. In these composites,the uniform increasing inhibition efficiency as the function of concentration deals with the adsorption phenomenon, the adsorption of inhibitors on the surface of MS is indicated by decrease in the double layer capacitanceand adsorption follows Langmuir adsorption isotherm. The percentage inhibition efficiency of composites obtained from potentiodynamic polarization and EIS measurements are in good agreement

References

1. Nandapure, B. I., Kondawar, S. B., Salunkhe, M. Y.,& Nandapure, A. I. (2013) Magnetic and transport properties of conducting Polyaniline/nickle oxide nanocomposites. Adv. Mat. Lett. 4, 134-140.
2. Nandapure, B. I., Kondawar, S. B., Salunkhe, M. Y., & Nandapure A. I. (2012) Proceedings of International Conference on Benchmarks in Engineering Science and Technology ICBEST .
3. Odonírio Abrahão Jr,Thiago Salem Pançonato Teixeira, João Marcos Madurro, Antonio Eduardo da Hora Machado, & Ana Graci Brito-Madurro, (2009) Quantum mechanical investigation of polymer formation from aminophenols.Journal of Molecular Structure: theochem. 913 (1), 28-37.
4. Chetouani, A., Medjahed, K., Sid-Lakhdar, K.E., Hammouti, B., Benkaddour, M., &Mansri, A. (2004)Poly (4-vinylpyridine-poly (3-oxide-ethylene) tosyle) as an inhibitor for iron in sulphuric acid at 80˚ C. Corros. Sci. 46, 2421–2430.
5. Tebbji, K., Bouabdellah, I., Aouniti, A., Hammouti. B., Oudda, H., Benkaddour, M., &Ramdani, A. (2007) N-benzyl-N-N-bis (3,5-dimethyl)-1H-pyrazol-1-yl)methyl 1 amine as corrosion inhibitor of steel in 1M Hcl. Mater. Lett. 61, 799–804.
6. Ebenso, E.E., & Oguzie, E.E. (2005) Corrosion inhibition of mild steel in acidic media by some organic dyes. Mater. Lett. 59, 2163–2165.
7. Kern, P.,Landolt, D.(2001) Adsorption of organic corrosion inhibitors on the iron in the active and passive state. A replacement reaction between inhibitor and water studies with the rotating quartz crystal microbalance. Electrochim. Acta. 47, 589-598.
8. Srikanth, A.P., Sunitha, T.G., Raman, V., Nanjundan, S., &Rajendran, N. (2007) Synthesis, characterization and corrosion protection properties of poly(*N*-(acryloyloxymethyl) benzotriazole-*co*-glycidyl methacrylate) coatings on mild steel. Mat.Chem.Phy. 103 (2) 241-247.
9. Elmansouri, A., Outzourhit, A., Lachkar, A., Hadik, N., Abouelaoualim, A., Achour, M.E., Oueriagli, A.,&Ameziane, E.L. (2009) Influence of the counter ion on the properties of poly(o-toluidine) thin films and their Schottky diodes. Syn. Met. 159 (3) 292-297.
10. Thenmozhi, G., &Jaya Santhi, R. (2014) Characterization, AC Conductivity and Dielectric behavior of chemically synthesized poly meta-Aminophenol. International Journal of Science and Research. 3 (9) 378-384.
11. Kar, P., Pradhan, N.C., & Adhikar, B. (2010) Induced doping by sodium ion in poly (*m*-aminophenol) through the functional groups. Synth. Met. 160 (13) 1524-1529.
12. Yang, S.H., Nguyen, T.P., Le Rendu, P., & Hsu, C.S. (2005) Optical and electrical properties of PPV/SiO_2 and PPV/TiO_2 composite materials. Compos. Part A: Appl. Sci. Manuf. 36 509–513.
13. Nag, M., Basak, P., & Manorama, S.V. (2007) Low-temperature hydrothermal synthesis of phase-pure rutile titania nanocrystals: Time temperature tuning of morphology and photocatalyst activity.Mater. Res. Bull.42 (9) 1691-1704.
14. Zhitao Li, Li Ma, Mengyu Gan, Wei Qiu, Dandan Fu, Sha Li,& Youqian Bai, (2013) Synthesis and anticorrosion performance of poly(2,3-dimethylaniline)–TiO_2 composite.Prog Org. Coat. 76 1161– 1167.

15. Thenmozhi, G., Mohanraj, G., Madhusudhana, G.,&Jayasanthi, R. (2014) Poly meta-Aminophenol: Chemical synthesis, Characterization and Ac Impedance study. *Journal of polymers. Article* ID 827043 11 pages.
16. Jia, W., Segal, E., Kornemandel, D., Lamhot, Y., Narkis, M., &Siegmann, A. (2002)Polyaniline-DBSA/organophilic clay nanocomposites: Synthesis and characterization. Synth. Met. 128 (1)115-120.
17. Zheng, J., Li, G., Ma, X., Wang, Y., Wu, G.,&Cheng, Y. (2008) Polyaniline–TiO_2 nanocomposite- based trimethylamine QCM sensor and its thermal behaviour studies, Sens. Actuators B: Chem. 2 (133) 374–380.
18. Thenmozhi, G., Arockiasamy, P., & Jaya Santhi R. (2014) Isomers of Poly Amino phenol: Chemical synthesis, Characterization and its corrosion protection aspect on Mild steel in 1M HCl. *International Journal of Electrochemistry*. Article ID 961617 11 pages.
19. Evrim Hur, Gozen Bereket, Berrin Duran, Derya Ozdemir, &Yucel Sahin. (2007) Electropolymerization of *m*-aminophenol on mild steel and its corrosion protection effect.Prog Org Coat. 60, 153-160.
20. Bereket, G., & Hur, E. (2009)The corrosion protection of mild steel by single layered polypyrrole and multilayered polypyrrole/poly(5-amino-1-naphthol) coatings. Prog Org Coat. 65 116-124.
21. Ahmed M Al-Sabagh, Notaila M Nasser, Ahmed A Farag, Mohamed A Migahed, Abdelmonem M F Eissa,&Tahany Mahmoud.(2013)Structure effect of some amine derivatives on corrosion inhibition efficiency for carbon steel in acidic media using electrochemical and Quantum Theory Methods. *Egyptian Journal of Petroleum.* 22 (1) 101–116.
22. Migahed, M.A.,Farag, A.A.,Elsaed, S.M.,Kamal, R., Mostfa, M.,&Abd El-Bary, H. (2011) Synthesis of a new family of Schiff base nonionic surfactants and evaluation of their corrosion inhibition effect on X-65 type tubing steel in deep oil wells formation water. Mater. Chem. Phys. 125 125–135.
23. Bentiss, F., Traisnel, M., &Lagrenee, M. (2000) The substituted 1, 3, 4-oxadiazoles: a new class of corrosion inhibitors of mild steel in acidic media. Corros. Sci.42 127-146.
24. Murlidharan, S.,Phani, K.L.N.,Pitchumani, S., Ravichandran, S., & Iyer, S.V.K. (1995) Polyamino-Benzoquinone Polymers: A New Class of Corrosion Inhibitors for Mild Steel. J. Electrochem. Soc.1421478-1483.
25. Arockiasamy, P., Queen Rosary Sheela, X., Thenmozhi, G., Franco, M., Wilson Sahayaraj, J., &Jaya Santhi, R., *International Journal of Corrosion.Article* ID 679192 7 pages.
26. *Gopalakrishnan Aridoss, Min Sung Kim, Se Mo Son, Jong Tae Kim,& Yeon Tae Jeong. (2010) Synthesis of poly(p-phenylenediamine-co-o-aminophenol)/multi-walled carbon nanotube composites by emulsion polymerization.Adv.Polym.Tech.21(12) 881-887.*
27. Quraishi, M.A., Rawat, J., & Ajmal, M. (2000) Dithiobiurets: a novel class of acid corrosion inhibitors for mild steel. J.Appl.Electrochem.30 745-751.

How to cite this article:

G. Thenmozhi and Jaya Santhi R., 2019,Synthesis of Poly P-Aminophenol/Tio2 Composite in the Presence of Anionicsurfactants and the Investigation of Anticorrosion Properties. *Int J Recent Sci Res.* 10(05), pp. 32283-32289.
DOI: http://dx.doi.org/10.24327/ijrsr.2019.1005.3437

****